Capsule-like CdS-modified TiO_2 nanocomposites with enhanced photodegradation under visible light irradiation

Xiaojie Song[1,2], Fan Yang[3], Qunling Fang[4], Hanmei Hu[1], Liuqian Sun[1]

[1]*School of Materials and Chemical Engineering, Anhui Jianzhu University, Hefei 230601, People's Republic of China*
[2]*School of Resources and Environmental Engineering, Anhui University, Hefei 230009, People's Republic of China*
[3]*Department of Chemistry, Anhui Medical University, Hefei 230026, People's Republic of China*
[4]*School of Medical Engineering, Hefei University of Technology, Hefei 230009, People's Republic of China*
E-mail: fyang99@mail.ustc.edu.cn

Published in Micro & Nano Letters; Received on 14th September 2014; Revised on 28th October 2014; Accepted on 30th October 2014

Novel cadmium sulfide (CdS)/titanium dioxide (TiO_2) nanocomposites with uniform 'capsule-like' distribution of CdS nanocrystals on TiO_2 nanoparticles (NPs) were successfully prepared by the hydrothermal method and the hot-injection method. The CdS/TiO_2 nanocomposites were characterised by X-ray powder diffraction, Fourier transform infrared spectroscopy, transmission electron microscopy, high-resolution transmission electron microscopy and scanning electron microscopy. The CdS/TiO_2 nanocomposites (with Ti/Cd mass ratio of 1:1) exhibited excellent photocatalytic activity in the degradation of rhodamine B in water compared with pure TiO_2 NPs and CdS NPs under visible light. The product might have potential applications in the cleanup of the environment because of its excellent photocatalytic activity.

1. Introduction: There are abundant water resources on the Earth, but with the rapid increase of population and industrial pollution in developing countries, clean water is becoming sparse and expensive. In the face of water shortage, thousands of tons of industrial and domestic waste water still pour into rivers and lakes [1]. Without any treatment, this contaminated water will directly harm the health of people. Nowadays, many new technologies such as bacterial flocculation, membrane adsorption [2–4] and the photocatalytic oxidation process [5] were developed and adopted in wastewater treatments.

Owing to their large specific area and high reactivity, nanophotocatalysts have been widely studied for decades as an ideal substitute for traditional wastewater treatments. Among the several common photocatalysts (titanium dioxide (TiO_2) [6–9], zinc oxide (ZnO) [8, 10], cadmium sulfide (CdS) [9] and silver nanoparticles (NPs) [11]), nanoTiO_2 is the best alternative because of its excellent photocatalytic activity, chemical and biological inertness and low cost [12, 13]. It has been employed to degrade several types of organic and inorganic pollutants in wastewater or on the surface of the adsorbent.

However, there are two critical disadvantages: wide bandgap and fast recombination of electron–hole pairs, which restrict the use of TiO_2 as a photocatalyst [14, 15]. The bandgap of titanium dioxide is 3.2 eV for anatase and 3.0 eV for rutile, respectively, and each of them is too wide to adsorb most of the solar radiation, especially the visible light. In addition, the efficiency of photogenerated electrons is high enough, but the high recombination of electron–hole pairs also lowers the photodegradation ability of TiO_2. To enhance photocatalysis efficiency and usage of visible light, many kinds of NPs have been used to dope with TiO_2 to prepare TiO_2-based photocatalysts. These materials, such as dye-sensitised material [16, 17], Ag, CuO_2 [18], CuS [19] and CdS [20, 21], can help TiO_2 to utilise both ultraviolet light (200–400 nm) and visible light (400–760 nm) [14] and reduce the recombination rate effectively.

Among these materials, nanoCdS is an ideal alternative because of its easy synthesis, effective usage of visible light and low recombination rate of electron–hole pairs. The narrow bandgap (2.4 eV) of CdS can help TiO_2 to extend the adsorption range of sunlight and the structure of the heterojunctions plays a vital role in the excitation, transportation and ultimate rate of the charge carriers. In this reported work CdS was doped with TiO_2 by a simple hydrothermal method to prepare visible light-driven photocatalysts. The capsule-like shape of CdS and the photocatalysis capacity of TiO_2/CdS was studied under visible light.

2. Experimental

2.1. Materials: Tetrabutyl titanate (TBT), acetic acid (HAc), sodium dodecyl sulfate (SDS), cadmium chloride-1-hydrate ($CdCl_2{\cdot}H_2O$), nitric acid (HNO_3), ammonia, sodium sulfide (Na_2S) and rhodamine B (RhB) were purchased from Sigma-Aldrich Corporation. All chemicals were of reagent grade and used without further purification.

2.2. Synthesis of TiO_2 NPs: TiO_2 NPs were synthesised by the following methods: 35 ml of ethanol, 10 ml of TBT and 3 ml of HAc were added into a 100 ml beaker in turn, and the solution was stirred for 0.5 h and named solution A. In 15 ml of anhydrous ethanol, 3 ml of the solution was stirred and named solution B. Solution B was added into solution A drop by drop with vigorous stirring; the pH of the mixture was adjusted to 9 using ammonia solution and the mixed solution was kept at 40°C for 2–3 h. The product was collected, rinsed with deionised water repeatedly and dried at 80°C. Finally, the product was calcined at 450°C for 2 h to remove residual organics.

2.3. Synthesis of capsule-like CdS-modified CdS/TiO_2 nanocomposites: 0.5053 g of as-synthesised TiO_2 NPs and 10 ml of 1% SDS solution were mixed and sonicated for 3 h to produce a uniform dispersion, and then 20 ml of 0.05 mol/l $Cd(NO_3)_2$ solution and 20 ml of 0.05 mol/l Na_2S solution were added drop by drop in turn. The mixture was stirred for 2 h, transferred into a 50 ml stainless steel reactor and heated to 180°C for 24 h. The yellow product was collected, washed with deionised water and dried.

For comparison, pure CdS NPs were also prepared through the aforementioned method.

2.4. Photocatalytic activity test: The photocatalytic degradation of RhB dye under visible light (100 mW/cm^2, radiation wavelength ≥420 nm) was carried out at room temperature. Typically, 150 mg of the sample was mixed with 50 ml of 25 mg/l RhB in a 100 ml

© The Institution of Engineering and Technology 2015

glass beaker, and the mixture was stirred for 2 h to attain adsorption equilibrium in the dark. After that, the mixture was irradiated under a visible light simulator while all other light sources were closed. A measure of 1 ml of photoreacted solution was extracted from the mixture at regular intervals, diluted to 10 ml and centrifuged at 16000 rpm/min for 5 min. The supernatant liquid was analysed using a UV–vis spectrometer to determine the degradation efficiency (C/C_0, C_0 and C were the initial concentration and residual concentration of RhB in the solution).

2.5. Characteristic: Fourier transform infrared spectroscopy (FTIR) spectra were recorded on an EQUINOX55 spectrometer (Bruker, Germany) using KBr pellets. The surface morphology and the elemental composition of the sample were characterised by scanning electron microscopy (SEM) (JEOL JBM-7500F, Japan) and high-resolution transmission electron microscopy (HRTEM) (JEOL-2010, Japan). The crystal phase of the sample was carried out using an X-ray diffractometer (Rigaku TTR-3, Japan) with Cu Ka radiation ($\lambda = 0.15418$ nm, $U = 60$ kV and $I = 300$ mA) in the 2θ range from 10° to 70°.

3. Results and discussion

3.1. X-ray powder diffraction (XRD) analysis: The XRD pattern of the CdS/TiO_2 nanocomposites is shown in Fig. 1. The diffraction peaks at 2θ of 25.3°, 37.8, 48.1° and 53.9° are attributed to (1 0 1), (0 0 4), (2 0 0) and (1 0 5) planes of anatase TiO_2 (JCPDS Card No. 21-1272). In addition, the diffraction peaks at 2θ of 25.0°, 26.5°, 28.2°, 43.6°, 47.8° and 51.8° are attributed to (1 0 0), (0 0 2), (1 0 1), (1 1 0), (1 0 3) and (1 1 2) planes of hexagonal wurtzite CdS (JCPDF 80-0006), respectively. These characteristic peaks indicate the formation of CdS and TiO_2 NPs.

3.2. Morphological analysis: To clarify the morphology and composition of NPs, TEM, SEM and HRTEM analyses are used. The TEM images of CdS NPs and CdS/TiO_2 nanocomposites are shown in Figs. 2*a* and *b*. Capsule-like CdS NPs with regular shapes and an average length of 40 nm and diameter of 30 nm can be observed in Fig. 2*a*, and there are other particles with irregular shapes besides the capsule-shaped ones in Fig. 2*b*. The different shapes indicate that there are different kinds of particles, so these particles with sizes of 15–20 nm should be TiO_2 NPs.

Fig. 2*c* shows the SEM image of CdS/TiO_2 nanocomposites. There are a large number of NPs which cluster together, some with small size, which should be TiO_2 and other global large particles, which should be the end of capsule-like CdS NPs.

Fig. 2*d* shows the typical HRTEM image of the CdS/TiO_2 nanocomposites, and the well-resolved two-dimensional lattice fringes of the material can be observed clearly. The interplanar spacing is measured carefully from the lattice fringes and compared with the JCPDS data. The lattice spacings of 0.359 and 0.352 nm measured from Fig. 2*d* correspond to the CdS (1 0 0) planes of the hexagonal wurtzite structure and the TiO_2 (1 0 1) planes of the anatase structure, respectively, and the distinct juncture between the two crystal phases can also be distinctly observed. The EDS spectrum obtained from the selected area in Fig. 2*d* confirms the absence of four elements (Ti, O, Cd and S). These results all confirm the formation of CdS and TiO_2 NPs and close attachment with each other, and are in accordance with XRD analysis.

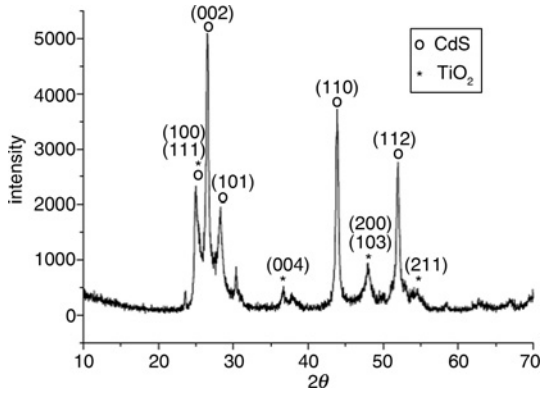

Figure 1 *XRD pattern of CdS/TiO_2 nanocomposites*

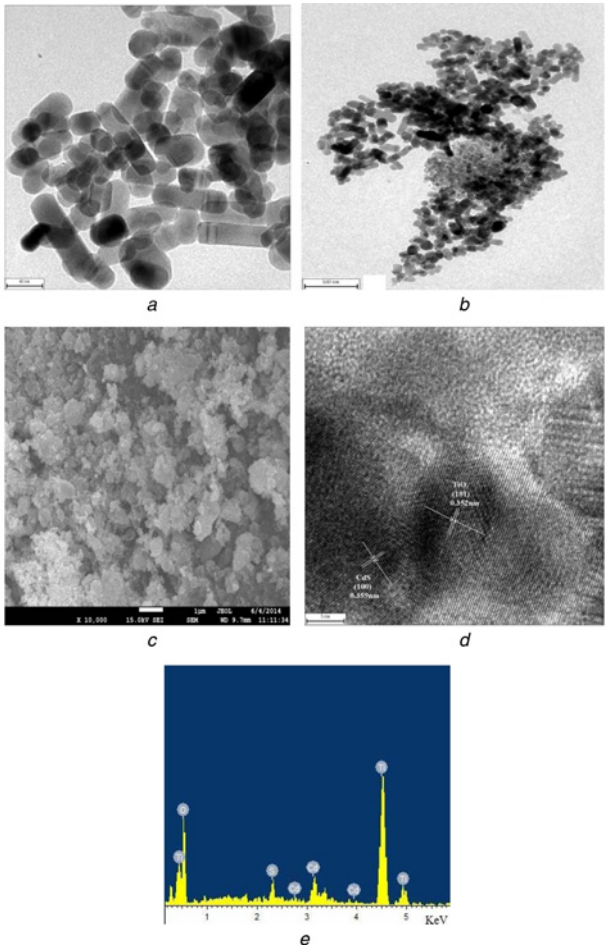

Figure 2 *TEM images of Cds NPs and Cds/TiO_2 nanocomposites; SEM, HRTEM and EDS image of Cds/TiO_2 nanocomposites*
a TEM images of CdS NPs
b TEM images of CdS/TiO_2 nanocomposites
c SEM image of Cds/TiO_2 nanocomposites
d HRTEM image of Cds/TiO_2 nanocomposites
e EDS image of CdS/TiO_2 nanocomposites

3.3. FTIR analysis: The FTIR spectra of CdS NPs, CdS/TiO_2 nanocomposites and TiO_2 NPs are shown in Fig. 3. The peaks at 3400, 2900 and 1600 cm^{-1} in curve *a* of the CdS NPs also appear in curve *b* of the CdS/TiO_2 nanocomposites. The peak at 1430 cm^{-1} in curve *b* is in accordance with the characteristic peak of the TiO_2 in curve *c*, which is attributed to Ti–O stretching.

3.4. Photocatalytic results and mechanism: Fig. 4 shows the photocatalytic degradation results of RhB under visible light for 200 min. Compared with the blank experiment, the three types of NPs exhibit different photocatalytic capacities. The catalytic capacity of TiO_2 is the weakest of the three types of NPs, and the capacity of the CdS/TiO_2 nanocomposites is a little greater than that of the CdS NPs. After 200 min of irradiation, the degradation rate of RhB by the CdS/TiO_2 nanocomposites is more than 97%,

© The Institution of Engineering and Technology 2015

doi: 10.1049/mnl.2014.0491

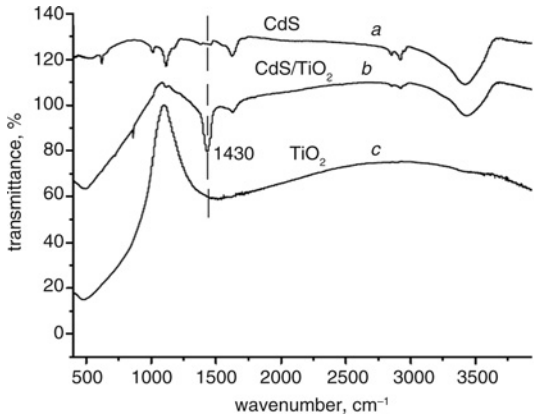

Figure 3 *FTIR spectra of CdS NPs (curve a), CdS/TiO_2 nanocomposites (curve b) and TiO_2 NPs (curve c)*

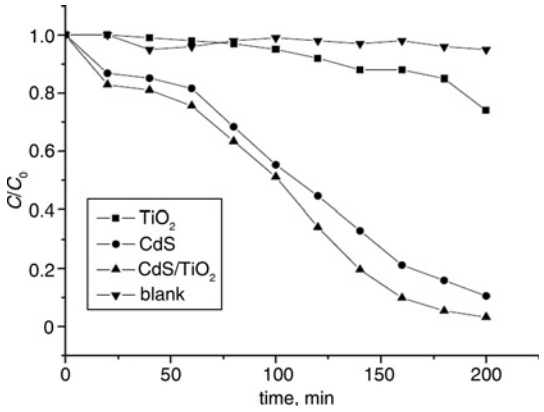

Figure 4 *Photocatalytic degradation of RhB (initial concentration = 25 mg/l, 50 ml) under visible light by TiO_2, CdS NPs and CdS/TiO_2 nanocomposites (after 2 h adsorption)*

and the degradation capacities of the CdS and TiO_2 NPs are 90 and 25%, respectively.

Pure anatase TiO_2 can only adsorb ultraviolet light whose wavelength is less than 387 nm, so it cannot utilise much of the sunlight. The forbidden band of pure CdS (2.4 eV) is less than that of anatase TiO_2 (3.2 eV), which means that CdS can utilise a broader range of sunlight. In our studies, the photocatalysis capacity of pure CdS is indeed stronger than TiO_2 under sunlight, but it is not the best. When the electrons are excited by the visible light from the valence band into the conduction band, the recombination of electron–hole pairs is also in process. Owing to this, the number of charge carriers (electrons and holes) is extremely limited in pure semiconductors. Doping moves either the conduction or valence band much closer to the Fermi level, and greatly increases the number of charge carriers (electrons and holes) (Fig. 5). Doping also helps to transfer the charges from CdS to TiO_2 through the conduction band, and realise the photocatalysis of TiO_2 under visible light. Through different reactions, both electrons in TiO_2 [22] and holes in CdS [23] can generate the superoxide radical anions ($O_2^{-}\bullet$) and hydroxyl radical ($\bullet$OH), which can react with the dye molecules and lead to the thorough degradation of the dye molecules. These all effectively enhance the photocatalysis capacity of TiO_2/CdS.

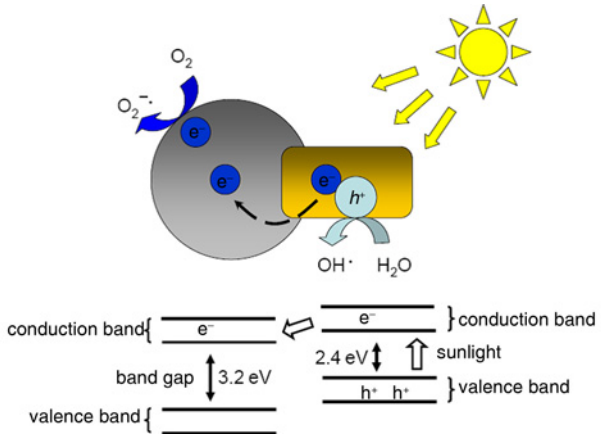

Figure 5 *Schematic diagram of the separation of generated electrons and holes on the interface of CdS/TiO_2 nanocomposites under visible light irradiation*

4. Conclusions: Capsule-like CdS NPs are successfully doped with TiO_2 NPs through the hydrothermal method. The nanocomposties are characterised by XRD, SEM, TEM, HRTEM, EDS and FTIR analysis, and the results show the synthesis of anatase TiO_2 and CdS. In morphological analysis, the size and shape of TiO_2 and CdS are uniform and the Cds are capsule-shaped. In photocatalytic study, TiO_2/CdS nanocomposites show outstanding photocatalysis capacity under visible light, and their photocatalysis capacity is obviously better than single TiO_2 NPs and CdS NPs. This is because of the doping of CdS on TiO_2 and advances the application of TiO_2/CdS in wastewater treatments.

5. Acknowledgments: This work was supported by the National Natural Science Foundation for Young Scholars (no. 21205026) and the Anhui Province Natural Science Foundation (no. 1508085QB38).

6 References

[1] Elimelech M., Phillip W.A.: 'The future of seawater desalination: energy, technology, and the environment', *Science*, 2011, **333**, pp. 712–717

[2] Shannon M.A., Bohn P.W., Elimelech M., Georgiadis J.G., Marinas B.J., Mayes A.M.: 'Science and technology for water purification in the coming decades', *Nature*, 2008, **452**, pp. 301–310

[3] Chong M.N., Jin B., Chow C.W., Saint C.: 'Recent developments in photocatalytic water treatment technology: a review', *Water Res.*, 2010, **44**, pp. 2997–3027

[4] Liu J., Bai H., Wang Y., Liu Z., Zhang X., Sun D.D.: 'Self-assembling TiO_2 nanorods on large graphene oxide sheets at a two-phase interface and their antirecombination in photocatalytic applications', *Adv. Funct. Mater.*, 2010, **20**, pp. 4175–4181

[5] Liu J., Liu L., Bai H., Wang Y., Sun D.D.: 'Gram-scale production of grapheme oxide–TiO_2 nanorod composites: towards high-activity photocatalytic materials', *Appl. Catal. B, Environ.*, 2011, **106**, pp. 76–82

[6] Hwang S.H., Song J., Jung Y., Kweon O.Y., Song H., Jang J.: 'Electrospun ZnO/TiO(2) composite nanofibers as a bactericidal agent', *Chem. Commun.*, 2011, **47**, pp. 9164–9166

[7] Li G.S., Zhang D.Q., Yu J.C.: 'A new visible-light photocatalyst: US quantum dotsembedded mesoporous TiO(2)', *Environ. Sci. Technol.*, 2009, **43**, pp. 7079–7085

[8] Bai H., Liu Z., Sun D.D.: 'Hierarchical ZnO/Cu corn-like materials with high photodegradation and antibacterial capability under visible light', *Phys. Chem. Chem. Phys.*, 2011, **13**, pp. 6205–6210

[9] Liu L., Liu J., Wang Y., Yan X., Sun D.D.: 'Facile synthesis of monodispersed silver nanoparticles on graphene oxide sheets with enhanced antibacterial activity', *New J. Chem.*, 2011, **35**, pp. 1418–1423

[10] Malato S., Fernández-Ibáñez P., Maldonado M.I., Blanco J., Gernjak W.: 'Decontamination and disinfection of water by solar photocatalysis: recent overview and trends', *Catal. Today*, 2009, **147**, pp. 1–59

[11] Zhang H., Chen G., Bahnemann D.W.: 'Photoelectrocatalytic materials for environmental applications', *J. Mater. Chem.*, 2009, **19**, pp. 5089–5121

© The Institution of Engineering and Technology 2015

[12] Herrmann J.M.: 'Heterogeneous photocatalysis: fundamentals and applications to the removal of various types of aqueous pollutants', *Catal. Today*, 1999, **53**, pp. 115–129
[13] Wang J., Tafen D.N., Lewis J.P., *ET AL.*: 'Origin of photocatalytic activity of nitrogen-doped TiO(2) nanobelts', *J. Am. Chem. Soc.*, 2009, **131**, pp. 12290–12297
[14] Gordon T.R., Cargnello M., Paik T., *ET AL.*: 'Nonaqueous synthesis of TiO_2 nanocrystals using TiF_4 to engineer morphology, oxygen vacancy concentration, and photocatalytic activity', *J. Am. Chem. Soc*, 2012, **134**, pp. 6751–6761
[15] Zhang M.A., Chen C.C., Ma W.H., Zhao J.C.: 'Visible-light-induced aerobic oxidation of alcohols in a coupled photocatalytic system of dye-sensitized TiO(2) and TEMPO', *Angewandte Chem. Int. Ed.*, 2008, **47**, pp. 9730–9733
[16] Zhao W., Sun Y.L., Castellano F.N.: 'Visible-light induced water detoxification catalyzed by Pt-II dye sensitized titania', *J. Am. Chem. Soc.*, 2008, **130**, pp. 12566–12567
[17] Zhu H., Tao J., Dong X.: 'Preparation and photoelectrochemical activity of Cr-doped TiO(2) nanorods with nanocavities', *J. Phys. Chem. C*, 2010, **114**, pp. 2873–2879
[18] Yang L.X., Luo S.L., Li Y., Xiao Y., Kang Q., Cai Q.Y.: 'High efficient photocatalytic degradation of p-nitrophenol on a unique Cu(2) O/TiO(2) p–n heterojunction network catalyst', *Environ. Sci. Technol.*, 2010, **44**, pp. 7641–7646
[19] Ratanatawanate C., Bui A., Vu K., Balkus K.J.: 'Low-temperature synthesis of copper(II) sulfide quantum dot decorated TiO_2 nanotubes and their photocatalytic properties', *J. Phys. Chem. C*, 2011, **115**, pp. 6175–6180
[20] Qi L., Yu J., Jaroniec M.: 'Preparation and enhanced visible-light photocatalytic H2-production activity of CdS-sensitized Pt/TiO_2 nanosheets with exposed (0 0 1) facets', *Phys. Chem. Chem. Phys.*, 2011, **13**, pp. 8915–8923
[21] Yang G.D., Yang B.L., Xiao T.C.: 'One-step solvothermal synthesis of hierarchically porousnanostructured CdS/TiO_2 heterojunction with higher visible lightphotocatalytic activity', *Appl. Surf. Sci.*, 2013, **283**, pp. 402–410
[22] Yang G.D., Yan Z.F., Xiao T.C., Yang B.L.: 'Low-temperature synthesis of alkalis doped TiO_2 photocatalysts and their photocatalytic performance for degradation of methyl orange', *J. Alloys Compd.*, 2013, **580**, pp. 15–22
[23] Xu F., Yuan Y., Han H., Wu D., Gao Z., Jiang K.: 'Synthesis of ZnO/CdS hierarchical heterostructure with enhanced photocatalytic efficiency under nature sunlight', *Cryst. Eng. Commun.*, 2012, **14**, pp. 3615–3622

© The Institution of Engineering and Technology 2015

doi: 10.1049/mnl.2014.0491